

Nuclear embedded star clusters in NGC 7582^{*}

M. Wold^{1†} and E. Galliano²

¹*European Southern Observatory, Karl-Schwarzschild str. 2, 85748 Garching bei München, Germany*

²*European Southern Observatory, Casilla 19001, Santiago 19, Chile*

Accepted 1988 December 15. Received 1988 December 14; in original form 1988 October 11

ABSTRACT

We report on the discovery of several compact regions of mid-infrared emission in the starforming circum nuclear disk of the starburst/Seyfert 2 galaxy NGC 7582. The compact sources do not have counterparts in the optical and near-infrared, suggesting that they are deeply embedded in dust. We use the [Ne II]12.8 μ m line emission to estimate the emission measure of the ionized gas, which in turn is used to assess the number of ionizing photons. Two of the brighter sources are found to have ionizing fluxes of $\sim 2.5 \times 10^{52}$, whereas the fainter ones have $\sim 1 \times 10^{52}$ photons s⁻¹. Comparing with a one Myr old starburst, we derive stellar masses in the range 3–5 $\times 10^5 M_{\odot}$ and find that the number of O-stars in each compact source is typically 0.6–1.6 $\times 10^3$. We conclude that the compact mid-infrared sources are likely to be young, embedded star clusters, of which only a few are known so far. Our observation highlights the need for high resolution mid-infrared imaging to discover and study embedded star clusters in the proximity of active galactic nuclei.

Key words: Galaxies: individual: NGC 7582; Galaxies: star clusters; Infrared: galaxies; Galaxies: Seyfert

1 INTRODUCTION

Starburst activity in nearby galaxies has, with the superior resolution of the Hubble Space Telescope (HST), been resolved into discrete massive young clusters since the pioneering work by Holtzman et al. (1992). In the literature, these clusters are usually referred to as super star clusters (SSC) or young massive clusters (YMCs). Their masses are typically $\geq 10^5 M_{\odot}$, radii ≤ 5 pc and ages ≤ 100 Myr. Most known young clusters in the Milky Way have masses below $\sim 10^4 M_{\odot}$ (Figer et al. 1999), but there also exist examples of YMCs in the Milky Way, such as the Westerlund 1 cluster which has a mass of $\sim 10^5 M_{\odot}$ (Clark et al. 2005). The most nearby analog to a YMC is the 30 Dor cluster in the Large Magellanic Cloud.

YMCs are blue compact sources, whose light is dominated by massive stars. As in the case of massive star association formation, the progenitors of YMCs are thermal radio sources deeply embedded in dust, e.g. the ultra dense H II regions, first discovered in Henize 2-10 by Kobulnicky & Johnson (1999). These objects are sources of mid-infrared (MIR) continuum and bright nebular line emission. Because of high dust extinction, they are usually very faint in the visible, and even in the near-infrared (NIR).

The first evidence for the existence of such MIR sources was unveiled by the Infrared Space Observatory (ISO) in the Antennae Galaxies NGC4038/9 (Mirabel et al. 1998). Most of the MIR flux from this galaxy complex comes from a small, optically insignificant, region. Subsequent NIR spectroscopy by Gilbert et al. (2000) suggests that the related cluster formed about 4 Myr ago, has a mass of $\approx 16 \times 10^6 M_{\odot}$, contains massive stars with T_{eff} up to 3.9×10^4 K, and is deeply embedded in dust, with $A_v \sim 10$.

Embedded YMCs have so far been observed in only a few galaxies: the Antennae and Henize 2-10, as already mentioned, NGC 5253 (Gorjian, Turner & Beck 2001), SBS 0335-052 (Plante & Sauvage 2002), IIZw40 (Beck et al. 2002) and NGC1808 and NGC1365 (Galliano et al. 2005).

Here we report on the discovery of bright, compact MIR sources in the composite starburst/Seyfert2 galaxy NGC 7582, using a VLT/VISIR image centered on the [Ne II]12.8 μ m emission line. We present the data in terms of suggestive evidence that the MIR sources are embedded YMCs, and use the [Ne II] luminosity to estimate physical properties, such as the number of ionizing photons and the number of massive stars within each source. We also emphasize that MIR imaging at high resolution is mandatory to study embedded star formation in the vicinity of active galactic nuclei (AGN).

^{*} Based on observations obtained with the ESO Very Large Telescope

[†] E-mail:mwold@eso.org

2 THE DATA

The data were obtained at the VLT-Melipal telescope with VISIR, a combined imager and spectrograph for observations in the *N* and *Q* bands (corresponding to the two atmospheric windows at 8–13 and 16.5–24.5 μm , respectively). A high-resolution spectrum and one narrow-band image centered on the [Ne II]12.8 μm line were obtained during the period September 29 to October 2, 2004. The VISIR detector is a SiAs 256 \times 256 DRS array, and a pixel scale of 0''.127 was used, yielding a field of view of 32''.5 \times 32''.5. Total integration time was one hour for both image and spectrum, and conditions on both nights were clear with humidity below 10%. The spectrum was taken in the high-resolution [Ne II]12.8 μm Echelle mode using a 0''.75 wide slit, giving a spectral resolution $R \approx 16000$, or $\approx 22 \text{ km s}^{-1}$. The diffraction limit is reached at 12.8 μm , hence both the spectrum and the image have the optimal spatial resolution of 0''.38. More details regarding the data are presented by Wold et al. (in preparation).

NGC 7582 has a redshift of $z = 0.00525$, hence one arcsec corresponds to $\approx 108 \text{ pc}$ in the galaxy rest frame¹, and the [Ne II] line is redshifted to 12.877 μm . The [Ne II] narrow-band filter has $\lambda_c = 12.81\mu\text{m}$ and half band width 0.21 μm , thus encompassing [Ne II] emission from the galaxy.

The [Ne II] narrow-band image displayed in Fig. 1 shows the central 6'' \times 6'' around the AGN. The MIR emission is resolved into several components, labelled M0–M6, where M0 corresponds to the AGN. There are two noticeably bright, dense knots of [Ne II] emission to the South, labeled M1 and M2. The central AGN is unresolved whereas the full width at half maximum (FWHM) of M1 and M2 are 0''.60 and 0''.65, respectively. M2 appears slightly extended in the SE–NW direction. The compact sources are themselves embedded in a larger and more diffuse envelope roughly 300–400 pc across. The position of the slit is indicated in the image, and the high-resolution spectrum of the [Ne II] line from M1 is shown to the left.

The measured fluxes and flux densities of the compact sources are listed in Table 1. The aperture diameters used correspond to 1 \times and 2 \times the diffraction-limited resolution. We estimated [Ne II] line fluxes from the narrow-band image by calibrating the image using the M1 line flux from the spectrum. The accuracy of the line fluxes derived from the narrow-band image in this manner is approximately 10 %. The spectrum shows that there is no continuum detected from M1. The noise level is $\approx 0.09 \text{ Jy}$, so the 3σ upper limit on the continuum is 0.27 Jy. By calibrating the narrow-band image using the M1 spectrum, we assume that the other sources M2–M6 also have non-detectable continua.

3 COMPARISON WITH DATA AT OTHER WAVELENGTHS

NGC 7582 is known to have a circum nuclear kpc-scale disk with active star formation, containing significant amounts of dust (Morris et al. 1985; Regan & Mulchaey 1999; Sosa-Brito et al. 2001). This is however the first time that the disk has been viewed at high resolution in the MIR,

Table 1. Measured quantities. Columns (2) and (3) show flux density within aperture diameters 0''.38 and 0''.76, respectively. Columns (4) and (5) show line flux, also within apertures of 0''.38 and 0''.76.

Source	[Ne II] flux density (mJy)		[Ne II] flux ($10^{-16} \text{ W m}^{-2}$)	
(1)	(2)	(3)	(4)	(5)
M1	45.3 \pm 4.5	131.2 \pm 7.7	1.5 \pm 0.1*	2.5 \pm 0.1*
M1	45.3 \pm 4.5	131.2 \pm 7.7	1.50 \pm 0.15	4.35 \pm 0.26
M2	43.9 \pm 4.5	126.7 \pm 7.6	1.46 \pm 0.15	4.20 \pm 0.25
M3	29.4 \pm 3.6	103.2 \pm 6.8	0.98 \pm 0.12	3.42 \pm 0.23
M4	29.0 \pm 3.6	95.9 \pm 6.6	0.96 \pm 0.12	3.18 \pm 0.22
M5	23.1 \pm 3.2	68.3 \pm 5.6	0.77 \pm 0.11	2.27 \pm 0.18
M6	17.6 \pm 2.8	59.7 \pm 5.2	0.59 \pm 0.09	1.98 \pm 0.17
Envelope**	2334.5 \pm 32.5	...	77.39 \pm 1.08	...

* Measured from the spectrum

** Aperture diameter 7''.62

and the nuclear starburst is resolved into several compact components embedded in a larger, more diffuse envelope. The compact sources, in particular M1 and M2, are reminiscent of young, massive, embedded star clusters. We searched the literature and various data archives in order to find counterparts to the MIR sources at other wavelengths, but no clear identifications can be made. A selection of data from optical to radio is shown in Fig. 2.

The top row of Fig. 2 shows two HST images, taken with WFPC2 and NICMOS through the *F606W* and *F160W* filters, respectively (programmes 8597 and 7330). Both HST images are dominated by stellar continuum, and the expected locations of M1 and M2 are marked with white open circles. No clear counterparts to M1 and M2 can be seen, and there is also no clear counterparts to the other fainter sources M3–M6.

Although no counterparts are found in continuum optical and NIR, there is extended emission from the starburst in narrow-band images centered on [Fe II]1.64 μm and Br γ at 2.165 μm (Sosa-Brito et al. 2001, fig. 3). [Fe II] traces shocks excited by supernova remnants (Vanzi & Rieke 1997), and indeed Reunanen, Kotilainen & Prieto (2003) observe a high [Fe II]/Br γ intensity ratio typical of shock excitation. This might indicate that the most massive stars in the starburst have already exploded as supernovae. The resolution in the [Fe II] and Br γ narrow-band images is however not as good as in the VISIR image, making it difficult to tell where the [Fe II] and Br γ emission comes from exactly. Some of it may come from the compact sources seen in the VISIR image, but it is also possible that a large contribution comes from the diffuse envelope.

The M2 source is clearly seen in the deconvolved 11.9 μm image by Siebenmorgen, Krügel & Spoon (2004), but M1 is either weak, or undetected. This morphology, with a weak or undetected M1 and a brighter M2 source, is also recognized in the narrow-band H₂ (2.12 μm) image by Sosa-Brito et al. (2001). A host-galaxy subtracted *L*-band image by Prieto, Reunanen & Kotilainen (2002) unveils part of the circum nuclear starburst disk, probably due to PAH emission at 3.3 μm .

The bottom row in Fig. 2 shows the VISIR image and an ATCA radio map obtained at 8.9 GHz (Morganti et al.

¹ We assume $H_0 = 70 \text{ km s}^{-1} \text{ Mpc}^{-1}$

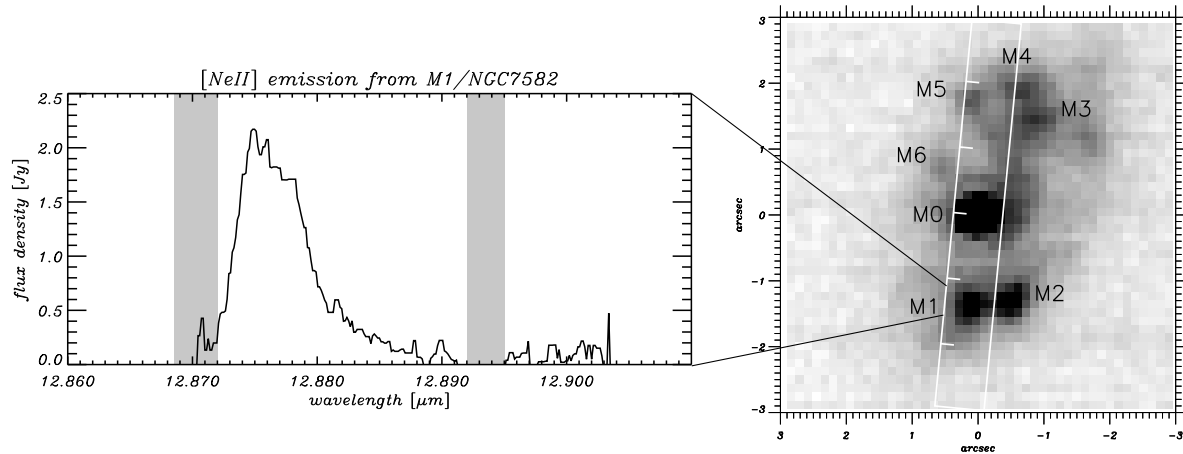


Figure 1. Narrow-band image and spectrum centered on the [NeII] line. The spectrum has not been continuum subtracted. The slit position is marked on the image. North is up and East is to the left.

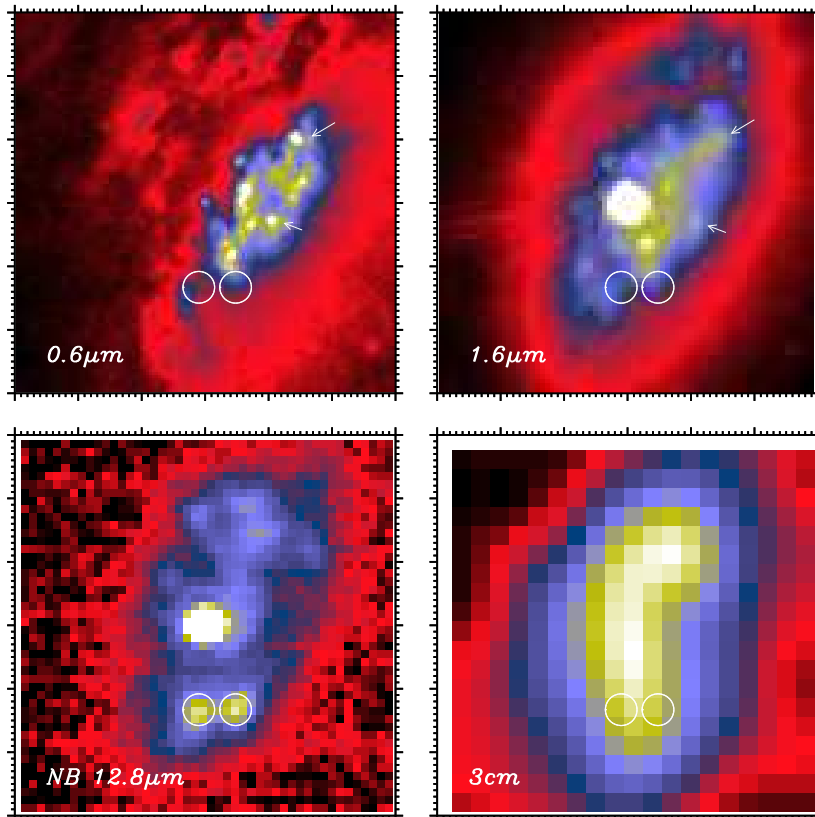


Figure 2. Comparison with data at other wavelengths. Top row, from left to right: HST/WFPC2 *F606W* and HST/NICMOS *F160W*. Bottom row, from left to right: the VLT/VISIR narrow-band image and a 3cm ATCA radio map. The two circles South of the nucleus indicate the location of the two MIR sources, M1 and M2. The two small arrows in the HST images point to the stars that were used for aligning. Each major tick mark corresponds to 1". North is up, and East is to the left.

1999). Young, dust-embedded star clusters are expected to show thermal free-free emission at radio wavelengths, but the resolution in the ATCA map is $\approx 1''$, not sufficient to match the resolution of the VISIR image. Extended emission from the starburst can clearly be seen, but part of the ra-

dio emission may also be non-thermal synchrotron emission from the AGN. When the Atacama Large Millimeter Array (ALMA) becomes available, it will be possible to separate the different components at mm and sub-mm wavelengths and study the starburst at great detail.

4 PHYSICAL PARAMETERS OF THE MIR SOURCES

[Ne II] is the most common Ne ion in H II regions, ionized by a broad range of stellar types. It is collisionally excited, and the line at 12.8 μm results from spontaneous radiative deexcitation. In typical star clusters, the electron density, n_e , is a factor of 10 or more lower than the critical density for collisional thermalization of the 12.8 μm transition, $n_c = 5.4 \times 10^5 \text{ cm}^{-3}$ (Johnson & Kobulnicky 2003). Because $n_e \ll n_c$, the emission measure of the ionized gas can be estimated from the [Ne II] line flux, which in turn can be used to predict the thermal free-free radio emission, the number of ionizing photons and the number of massive stars (Keto et al. 1999). We proceed along the lines of the analysis done by Keto et al. (1999), and calculate the emission measure by using that the [Ne II] line intensity depends on the number of atoms in the upper state:

$$I = 3 \times 10^{-8} \left(\frac{10^4 \text{ K}}{T_e} \right)^{\frac{1}{2}} \exp\left(-\frac{h\nu}{kT_e}\right) \int \frac{n_e}{(n_e + n_c)} \gamma_{\text{Ne}} n_e^2 dl \quad (1)$$

(Keto et al. 1999 and references therein²). The line intensity, I , has units of $\text{erg s}^{-1} \text{ cm}^{-2} \text{ sr}^{-1}$ and the emission measure, $EM = n_e^2 dl$, has units of $\text{cm}^{-6} \text{ pc}$. We assume electron temperature and density of $T_e = 10^4 \text{ K}$ and $n_e \ll n_c$, respectively, and that the abundance of Ne relative to H is $\gamma_{\text{Ne}} = 0.83$ (Keto et al. 1999). From the flux measurements in Table 1, we derive [Ne II] intensities by dividing with the solid angle, Ω , subtended by the source, taken to be equal to the area of the circular aperture used for photometry. Table 2 lists the derived emission measures.

The emission measure is directly related to the optical depth, τ_ν^{ff} , in the free-free continuum (Keto et al. 1999, eq. 4), and we estimate optical depths at 5 GHz of ≈ 0.01 – 0.02 . The optically thin approximation for brightness temperature, $T_b = T_e \tau_\nu^{\text{ff}}$, is therefore valid. We proceed with calculating the radio flux density at 5 GHz arising from free-free processes from the brightness temperature given that $S_\nu = 2\nu^2 k T_b / c^2 \Omega$, see third column of Table 2.

The Lyman continuum photon flux required to maintain ionization is given by

$$N_{\text{ph}} (\text{s}^{-1}) = 8.04 \times 10^{46} T_e^{-0.85} U^3. \quad (2)$$

The excitation parameter, U , can be written as

$$U = 4.533 \left[\left(\frac{\nu}{\text{GHz}} \right)^{0.1} \left(\frac{T_e}{\text{K}} \right)^{0.35} \left(\frac{S_\nu}{\text{Jy}} \right) \left(\frac{D}{\text{kpc}} \right)^2 \right]^{1/3} \quad (3)$$

(Kurtz, Churchwell & Wood 1994), where D is the distance to the source. Using the radio flux calculated above, we find that the number of ionizing photons in the compact MIR sources is $2 \times 10^{52} \text{ s}^{-1}$ as listed in the fourth column of Table 2.

Only massive O- and B-type stars contribute to the Lyman continuum flux, hence we can make an estimate of their numbers within each source. By making assumptions about the age of the compact sources and the initial mass function (IMF), we can also derive stellar composition and mass

of each source. In order to do this we run a Starburst99 (Leitherer et al. 1999; Vázquez & Leitherer 2005) model as an instantaneous starburst with a Kroupa IMF (Kroupa 2002) with low mass cut-off at 0.10 M_\odot and high-mass cut-off at 100 M_\odot . Assuming age of one million years, we find that the compact MIR sources contain 1000–1500 O-type stars. The total mass in stars of each source, including the stars that do not contribute to the ionizing flux, is typically 3 – $5 \times 10^5 M_\odot$. The total stellar mass (assuming an age of one Myr) and the number of O-stars in each source are listed in the last two columns of Table 2.

The numbers vary relatively little with the age of the model as long as the age is $\lesssim 4$ Myr. As the age increases, the Lyman continuum photon flux decreases, so more stars are required in order to produce the observed photon flux of $\approx 10^{52.4} \text{ s}^{-1}$. If the average photon flux per OB star is $10^{49} \text{ photons s}^{-1}$ (Smith, Norris & Crowther 2002; Martins, Schaerer & Hillier 2005), the cluster cannot contain more than a few thousand OB stars, as derived above. But if the age is > 4 – 5 Myr, the cluster must contain more OB stars and hence be more massive.

If we assume that all the ionizing flux eventually is emitted into the infrared, we can calculate an upper limit to the MIR continuum. For this, we use eqs. A2 and A3 from Genzel et al. (1982) which assume that the dust emission can be approximated by a grey body radiating at 300 K. The predicted upper limits at 12.8 μm , labeled S_{MIR} in Table 2, are consistent with our measured 3σ upper limit of 0.27 Jy.

The radio flux from the central regions of NGC 7582 consists of contributions from thermal free-free emission from the starburst, synchrotron radiation from supernova remnants and the AGN. The radio flux we derive above is, by definition, due to thermal free-free emission and we can compare the predicted thermal radio emission with the observed flux to estimate the contribution from non-thermal processes. As existing radio measurements cannot resolve the different MIR components, we compare with the estimated thermal radio flux for the whole envelope (on the last line of Table 2). At frequencies of 8.6, 4.9 and 1.4 GHz we derive free-free continuum fluxes of 33.6, 29.7 and 28.1 mJy, respectively. The measured radio fluxes at the same frequencies are 49.29, 69 and 166 mJy (Ulvestad & Wilson 1984; Morganti et al. 1999). The contribution from free-free emission related to the starburst is therefore ≈ 20 , 40 and 70% in order of increasing frequency. The relative contribution from free-free processes increases with frequency because, as opposed to synchrotron emission, free-free processes produce almost flat radio spectra. We have assumed that there is little synchrotron contribution from supernovae. If the age is small enough that not many supernovae have exploded yet, this is a valid assumption. However, there may be contributions to synchrotron emission from supernovae in the envelope. The observed extended [Fe II] emission (Sosa-Brito et al. 2001) may indicate that some supernovae have already occurred. It is however possible that the compact sources are younger than the surrounding envelope.

² The constant 3×10^8 in Keto et al.'s eq. 2 is probably a typing error, and should be 3×10^{-8} as used here.

Table 2. Derived quantities of the sources. The size of the envelope is taken to be equal to the area of a circle with $7''.62$ diameter.

Source	EM $\times 10^6 \text{ cm}^{-6} \text{ pc}$	S_{5GHz}^{ff} mJy	$\log N_{\text{ph}}$ s^{-1}	S_{MIR} mJy	$\log M_{\text{tot}}$ M_{\odot}	$\log N$ O-stars
M1	2.51	0.58	52.39	21.76	5.71	3.21
M2	2.44	0.56	52.38	21.11	5.69	3.19
M3	1.63	0.37	52.20	14.14	5.52	3.02
M4	1.61	0.37	52.20	13.93	5.51	3.01
M5	1.28	0.29	52.10	11.10	5.41	2.92
M6	0.98	0.22	51.98	8.49	5.30	2.80
Envelope	0.32	29.69	54.10	1122.50	7.42	4.92

5 CONCLUSIONS

We have detected several compact regions of $[\text{Ne II}]12.8\mu\text{m}$ emission in the circum nuclear starburst disk of NGC 7582. The compact MIR sources are embedded in a larger and more diffuse envelope 300–400 pc across, and do not have counterparts detected at continuum optical and NIR wavelengths. If the sources are young star clusters, the compact MIR emission suggests they are embedded in their own dusty birth material. The MIR emission of young, embedded clusters is expected to decrease as the most massive stars explode as supernovae and gas and dust are expelled. That the sources are bright in the MIR, and with no counterparts detected in continuum optical or NIR, suggests they may be young. It can however not be excluded that the clusters could be older and obscured by a screen of dust related to the circum nuclear disk.

We estimate that the number of ionizing photons within each compact source is $1\text{--}2.5 \times 10^{52} \text{ s}^{-1}$. By comparing with starburst models we find that the stellar mass of the two brighter sources M1 and M2 probably is $\sim 5 \times 10^5 M_{\odot}$ and that they each contain roughly 1.5×10^3 O-type stars. The less bright sources M3–M6 probably have smaller masses of $2.0\text{--}3.2 \times 10^5 M_{\odot}$ and contain $\sim 1.0 \times 10^3$ O-type stars. These properties are very similar to those of young, embedded star clusters (Keto et al. 1999; Gorjian et al. 2001; Johnson & Kobulnicky 2003).

Our observation highlights the need for high-resolution MIR imaging and spectroscopy to study nuclear starbursts and individual embedded star clusters in circum-AGN environments.

ACKNOWLEDGMENTS

We are grateful to the VISIR Science Verification team, to M. Lacy, A. Bik and S. Larsen for helpful discussions, and to D.J. McKay for the archival ATCA image. The referee is acknowledged for an insightful report.

REFERENCES

Beck S. C., Turner J. L., Langland-Shula L. E., Meier D. S., Crosthwaite L. P., Gorjian V., 2002, *AJ*, 124, 2516
 Clark J. S., Negueruela I., Crowther P. A., Goodwin S. P., 2005, *A&A*, 434, 949
 Figer D. F., Kim S. S., Morris M., Serabyn E., Rich R. M., McLean I. S., 1999, *ApJ*, 525, 750

Galliano E., Alloin D., Pantin E., Lagage P. O., Marco O., 2005, *A&A*, 438, 803
 Genzel R., Becklin E. E., Moran J. M., Reid M. J., Jaffe D. T., Downes D., Wynn-Williams C. G., 1982, *ApJ*, 255, 527
 Gilbert A. M., Graham J. R., McLean I. S., Becklin E. E., Figer D. F., Larkin J. E., Levenson N. A., Teplitz H. I., Wilcox M. K., 2000, *ApJ*, 533, L57
 Gorjian V., Turner J. L., Beck S. C., 2001, *ApJ*, 554, L29
 Holtzman J. A., Faber S. M., Shaya E. J., Lauer T. R., Groth J., Hunter D. A., Baum W. A., Ewald S. P., Hester J. J., Light R. M., Lynds C. R., O’Neil E. J., Westphal J. A., 1992, *AJ*, 103, 691
 Johnson K. E., Kobulnicky H. A., 2003, *ApJ*, 597, 923
 Keto E., Hora J. L., Fazio G. G., Hoffmann W., Deutsch L., 1999, *ApJ*, 518, 183
 Kobulnicky H. A., Johnson K. E., 1999, *ApJ*, 527, 154
 Kroupa P., 2002, *Science*, 295, 82
 Kurtz S., Churchwell E., Wood D. O. S., 1994, *ApJS*, 91, 659
 Leitherer C., Schaerer D., Goldader J. D., Delgado R. M. G., Robert C., Kune D. F., de Mello D. F., Devost D., Heckman T. M., 1999, *ApJS*, 123, 3
 Martins F., Schaerer D., Hillier D. J., 2005, *A&A*, 436, 1049
 Mirabel I. F., Vigroux L., Charmandaris V., Sauvage M., Gallais P., Tran D., Cesarsky C., Madden S. C., Duc P.-A., 1998, *A&A*, 333, L1
 Morganti R., Tsvetanov Z. I., Gallimore J., Allen M. G., 1999, *A&AS*, 137, 457
 Morris S., Ward M., Whittle M., Wilson A. S., Taylor K., 1985, *MNRAS*, 216, 193
 Plante S., Sauvage M., 2002, *AJ*, 124, 1995
 Prieto M. A., Reunanen J., Kotilainen J. K., 2002, *ApJ*, 571, L7
 Regan M. W., Mulchaey J. S., 1999, *AJ*, 117, 2676
 Reunanen J., Kotilainen J. K., Prieto M. A., 2003, *MNRAS*, 343, 192
 Siebenmorgen R., Krügel E., Spoon H. W. W., 2004, *A&A*, 414, 123
 Smith L. J., Norris R. P. F., Crowther P. A., 2002, *MNRAS*, 337, 1309
 Sosa-Brito R. M., Tacconi-Garman L. E., Lehnert M. D., Gallimore J. F., 2001, *ApJS*, 136, 61
 Ulvestad J. S., Wilson A. S., 1984, *ApJ*, 285, 439
 Vanzani L., Rieke G. H., 1997, *ApJ*, 479, 694
 Vázquez G. A., Leitherer C., 2005, *ApJ*, 621, 695

This paper has been typeset from a \TeX / \LaTeX file prepared by the author.